Available online at www.sciencedirect.com
SCIENCE DIRECT®
Polymer 45 (2004) 3819–3825
polymer
www.elsevier.com/locate/polymer

Effects of annealing (solid and melt) on the time evolution of polymorphic structure of PA6/silicate nanocomposites

Xiao Hu*, Xiongyan Zhao

Polymer Laboratory, School of Materials Engineering, Nanyang Technological University, Nanyang Avenue, Singapore 639798, Singapore

Received 8 October 2003; received in revised form 28 February 2004; accepted 18 March 2004

Abstract

The effects of annealing including solid-state annealing (190 °C) and melt-state annealing (230 and 250 °C) on the polymorphic behavior and thermal property of polyamide 6 (PA6)/layered-silicate nanocomposites (PA6LSN) have been investigated as a function of annealing time using Modulated Differential Scanning Calorimetry (MDSC) and wide angle X-ray diffraction. For comparison, thermal behavior and polymorphism of pure PA6 were also studied. It was demonstrated that PA6LSN and PA6 exhibited a similar polymorphic behavior when they were annealed in the solid state for different time duration. As the annealing temperature was elevated to 230 and 250 °C, significant differences in thermal behavior and polymorphism between PA6LSN and PA6 could be found. For example, the γ phase became the absolutely dominating for PA6LSN, while the α crystal was the most predominant phase in neat PA6. Moreover, a new endothermic peak is observed around 235 °C in all PA6LSN MDSC scans, which might be related to the melting of PA6 lamellae formed in the confined environment on the surface of the nano-silicate.

Keywords: Polyamide 6; Nano-composites; Crystal structure

1. Introduction

Fillers at nano-scale level show impressive promise in providing superior properties for multifunctional applications. The function of nano-clay as a stiffener is many times more effective than micro-scale inorganic fillers such as short glass fibres. The particle when properly exfoliated in about 1 nm in thickness with aspect ratios ranging from tens up to a thousand. The property improvements for organic–inorganic nanocomposites can generally be classified into the following aspects including (i) dramatically improved mechanical properties [1,2], (ii) heat resistance [3–5], (iii) dimensional stability [6], (iv) superior barrier to gas and water [6,7], and (v) flame retardation [8,9]. Thus, one of the exciting and promising developments in material science today is the design and synthesis of organic–inorganic nanocomposites that possess enhanced and novel properties, which are unattainable in the individual organic and inorganic materials [10–13].

With the development of polyamide6 (PA6)/clay nanocomposites by Tyoto Research Center [1,2], there have been increasing attentions to this system in the past decade [14–20]. As we know, one of the most remarkable features of PA6 is that this semicrystalline polymer exhibits polymorphism depending on the thermal history, processing conditions, mechanical stress, crystallization conditions and so on. Since the polymorphic form may have importany effect on thermal properties such as heat distortion temperature (HDT), softening, dimensional stability and warpage, polymorphism and polymorphic transformations of PA6 nanocomposites have drawn considerable research interests. Studies on the crystal structure of PA6 in nanocomposites were first carried out by Kojima et al. [21], who reported that both α and γ crystals were present in nanocomposites. However, after annealing under elevated pressure, they found that the fraction of γ-phase decreased. Mathias et al. [15] reported that while both crystal forms were present in nanocomposites, annealing at 200 °C under vacuum produced only γ crystals. On the other hand, Wu et al. [18] showed from his DSC and XRD results that the polymorphic behavior in nylon 6/clay nanocomposites is dependent on the content of clay and the cooling rate from the melt. High cooling rate from the melt result in the

* Corresponding author. Tel.: +65-6790-4610; fax: +65-6790-9081.
E-mail address: asxhu@ntu.edu.sg (X. Hu).

0032-3861/$ - see front matter © 2004 Elsevier Ltd. All rights reserved.
doi:10.1016/j.polymer.2004.03.055

formation of less stable γ crystalline phase. In addition, thermal treatment of PA 6 and PA 6/clay nanocomposites at various temperatures promotes mostly the α form crystalline formation. Although intensive research efforts have been devoted to this system, to the best of our knowledge, most research mainly focus on the effect of clay and the annealing temperature on crystallization behaviour of PA6 matrix [5,14–20,22,23], the effect of melt annealing on thermal behaviour of PA6/clay nanocomposites is still an interesting subject needed to be further investigated since some microstructural changes may occur at such high annealing temperatures, which would have a significant impact on properties of PA6/clay nanocomposites.

One of the objectives of this work is to investigate the effects of annealing conditions, especially annealing in the melt state, on the time evolution of the polymorphic structure of PA6 matrix in PA6/silicate nanocomposites and to understand whether and how the thermal history affects the thermal properties of nanocomposites. Moreover, one remarkable feature of this work is that a new endothermic peak is detected in PA6/silicate nanocomposite system for the first time. Therefore, another objective of this work is to investigate the effects of annealing on this new peak and also attempts to elucidate its physical origin. In particular, we will focus our attention on the comparative study of the thermal properties of pure PA6 and PA6/silicate nanocomposites.

2. Experimental

2.1. Materials

Polyamide 6 (PA6) and its layered-silicate nanocomposites with approximately 4 wt% clay (PA6LSN) were originally from Unitika, Ltd. (Japan) in the form of granular samples. The detailed material compositions are proprietary, but both are described as reactor grade in situ polymerized nanocomposites derived from a synthetic phillosilicate or mica nanofiller with octadecylamine treatment, or a similar long-chain aliphatic amine treatment. Earlier reports by Ellis et al showed that it has a fully exfoliated morphology [24,25]. The as-received samples were cut into small pieces and then dried under vacuum at 80 °C for 24 h prior to MDSC characterizations. For the XRD measurements, the dried samples were melted in a DSC cell under N_2 at 280 °C, and then pressed into thin sheets and kept for about 8 min to eliminate the thermal history of PA6. Finally, the samples were removed from the cell and cooled down to room temperature.

2.2. Characterization

A Modulated Differential Scanning Calorimeter (MDSC) (2920 Modulated DSC, TA Instrument) was used to analyze the thermal transition behavior of the samples. MDSC is a relatively new technique which subjects a sample to a linear heating ramp with a superimposed low frequency temperature oscillation (modulation) resulting in a modulation in the heating profile. It could provide a better insight into the study of complicated transition in polymers. In addition, the ability to study transitions at very low heating rates gives very high resolution that permits the detection of weak transition. All MDSC runs were made under a nitrogen atmosphere with heating rate of 5 °C/min, and the thermal histories, namely annealing temperature and annealing time, of the specimens were varied. The MDSC was carefully calibrated for temperature and heat flow following the standard procedures. The thermal transitions are reported as the maximum or minimum of the endothermic or exothermic peaks respectively. In order to avoid any influence of previous thermal history, every sample was used only once.

Wide-angle X-ray diffraction (WAXD) patterns were taken on a Rigaku RINT 2200 X-ray diffractometer (Cu K_α radiation at 40.0 kV and 30.0 mA). The range of 2θ measurement is 3–30° and scanning rate is 5°/min.

3. Results and discussion

Fig. 1 illustrates the total MDSC heat flow signals for the silicate, neat PA6 and as-received PA6/layered-silicate nanocomposites (PA6LSN). Upon heating from 50 to 280 °C, at a heating rate of 5 °C/min, only one peak appeared in neat PA6 DSC thermograms at 221.3 °C which should be associated with the α-form crystals of PA6 [14,16,26,27]. For PA6LSN, however, a quite different thermogram was observed as compared with that of neat PA6. It can be seen from Fig. 1 that three different transitions appeared in PA6LSN total MDSC thermograms. In addition to the presence of a sharp endothermic peak at 220.8 °C assignable to the melting of α-form crystals of PA6, another two endotherms were also detected. There are a broad and less pronounced endothermic shoulder around 200.8 °C, and a broad but distinct endothermic peak centered around 235.7 °C. The former is associated with the melting of

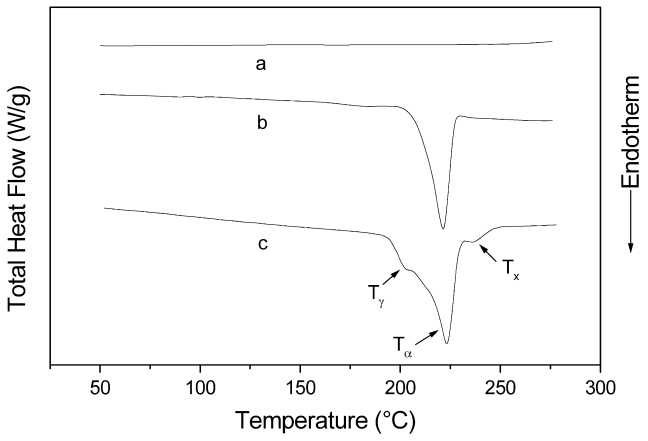

Fig. 1. MDSC thermograms of (a) silica, (b) pure PA6 and (c) PA6LSN.

γ-form crystals of PA6 [28], which suggests that the presence of layered silicates in PA6 is more inclined to promote the formation of γ-form crystals. This is because loading of silicates has a strong heterophase nucleation effect, which is favorable for the formation of γ-form crystals [5,16,23]. A remarkable feature in Fig. 1 was the appearance of the new high-temperature endothermic peak around 235.7 °C in MDSC traces of PA6LSN. In fact this peak was seen in all MDSC scans carried out for the nano-composite. It is clear that this endothermic peak should be closely related to the addition of the layered-silicates into PA6 matrix. But evidently, such a new endothermic peak does not come from silicate itself, since no thermal transitions can be detected around this melting region from the MDSC thermograms of pure silicate (see Fig. 1). The possible physical origin about this new thermal transition will be discussed later. The different thermal events between neat PA6 and PA6LSN are seen more clearly in Fig. 2, which shows the non-reversing MDSC signal of both samples. For neat PA6, both exothermic and endothermic non-reversible events were detected simultaneously. There is a strong exotherm peaked at 203.6 °C immediately followed by a sharp endothermic peak at 221.6 °C, indicating that the α-phase crystals undergo a process of crystal perfection during the heating scan and subsequently these higher melting species melt at 221.6 °C. For sample PA6LSN, however, two crystalline perfection processes seem to have appeared in the non-reversing exothermic signal. There is a broad and pronounced exotherm overlapping with the melting endotherm. The first broad exotherm before melting seems to hint that it is probably due to the overlap of crystal perfection processes of both the α-phase and γ-phase. The exotherm after the melting might be related to the high-temperature melting peak (see Fig. 1). The difference in the non-reversing curves of MDSC data between neat PA6 and PA6LSN reflected the complexity of the melting behavior for PA6LSN system.

X-ray diffraction data also confirm the difference in the structural features between neat PA6 and PA6LSN. It can be seen from Fig. 3 that for neat PA6, two reflections have been observed at $2\theta = 20.5$ and 24.3° corresponding to α_1 and α_2, respectively. According to Murthy [29] $\alpha_1$orginates from the distance between hydrogen-bonded chains, while α_2 comes from the distance between hydrogen-bonded sheets. This indicates that the α-phase is the dominant crystalline phase for neat PA6. For as-received PA6LSN samples, however, in addition to the two reflections as seen in neat PA6, two other reflections are also detected at $2\theta = 10.8$ and 21.5°, which are related to γ_1 and γ_2 crystal planes of PA6 [14,16,30–32]. Thus, the addition of silicates into neat PA6 could favor the formation of γ-phase crystalline, which agrees well with the MDSC results. In addition, no diffraction peak is observed at low 2θ angle for the nano-composites. This corroborates well with the fully exfoliated morphology of this Unikita nano-composite prepared by in situ polymerization reported recently by Ellis et al. [24,25].

In order to distinguish the three endothermic peaks appeared in PA6LSN during heating run, their temperatures were defined as T_γ for the melting peak of γ-form crystals, T_α, for the melting peak of α-form crystals and T_x for the high-temperature unknown peak respectively. The corresponding enthalpies of melting transition were named as ΔH_γ, ΔH_α and ΔH_x, respectively.

Annealing studies were carried out at different temperatures (T_a) in order to have a deeper understanding of the differences between PA6 and PA6/layered-silicate nano-composites and the effect of thermal history on their phase behavior and structures. The samples, after eliminating the processing histories, were first heated to the annealing temperature at 40 °C/min, then maintained at this temperature for a given duration, and then cooled to the room temperature at the same rate (40 °C/min). Finally the sample was heated from room temperature to the designated temperature at the rate of 5°/min. In order to better investigate the thermal and crystal morphological properties during annealing, three different annealing temperatures were chosen carefully in this study, i.e., 190 °C (below T_γ, solid-state annealing), 230 °C (below T_x and above T_γ and

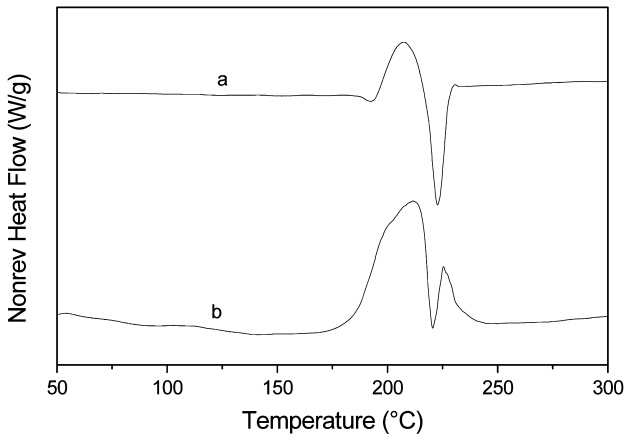

Fig. 2. Non-reversing heat flow curve of (a) pure PA6 and (b) PA6LSN.

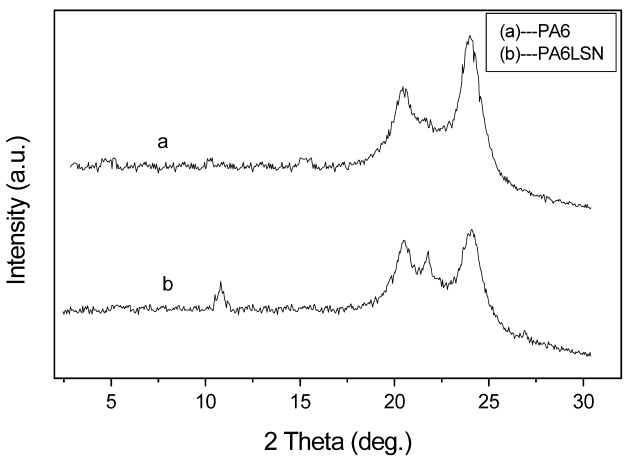

Fig. 3. Wide-angle X-ray diffraction patterns of (a) pure PA6 and (b) PA6LSN.

T_α, melt-state annealing I) and 250 °C (above T_x, melt-state annealing II).

Fig. 4 gives the traces of MDSC thermograms of PA6LSN specimens, after annealing at 190 °C for different durations of time. A fresh sample was used for each MDSC run. It can be seen in Fig. 4 that the peak temperature T_γ increases with increasing annealing time, but the other two transition temperatures (T_α and T_x) remain virtually unchanged regardless of the annealing time employed. Similar results for T_γ and T_α were also observed in the neat PA6 (Fig. 5). The increase in T_γ implies a corresponding increase in crystalline perfection of γ-form crystals with increasing annealing time, probably due to the fact that the longer annealing duration could provide more time to relieve the crystal defects. This is not surprising since, in solid state, polymer chains or segments are allowed to arrange themselves into a better organization when suitable conditions such as temperature and time are given in order to keep the system in a relatively lower energy. Fig. 6 shows the relationships between enthalpies of transition and logarithmic annealing time (log t). It is observed that ΔH_x for the high-temperature melting peak at about 230 °C shows little change with increasing annealing time. In other words, ΔH_x appeared unaffected by the annealing at 190 °C. However, ΔH_γ of the endothermic shoulder peak was found to increase with increasing annealing time and ΔH_α showed a slight decrease after annealing. The relative ratios between ΔH_γ and ΔH_α in neat PA6 and PA6LSN are illustrated clearly in Fig. 7, which compares the changes in $\Delta H_\gamma/(\Delta H_\alpha + \Delta H_\gamma)$ as a function of annealing time. When the annealing time is less than 60 min, the $\Delta H_\gamma/(\Delta H_\alpha + \Delta H_\gamma)$ values for PA6LSN samples are comparable to that of neat PA6 treated under the same conditions. However, as the annealing time exceeds 120 min, there is an abrupt increase in the $\Delta H_\gamma/(\Delta H_\alpha + \Delta H_\gamma)$ value for PA6SLN nanocomposite, while the $\Delta H_\gamma/(\Delta H_\alpha + \Delta H_\gamma)$ value of the neat PA6 still exhibits a gradual increase similar to that seen during the early stage of annealing. It has been reported that annealing can relieve some of the residual stress accumulated during

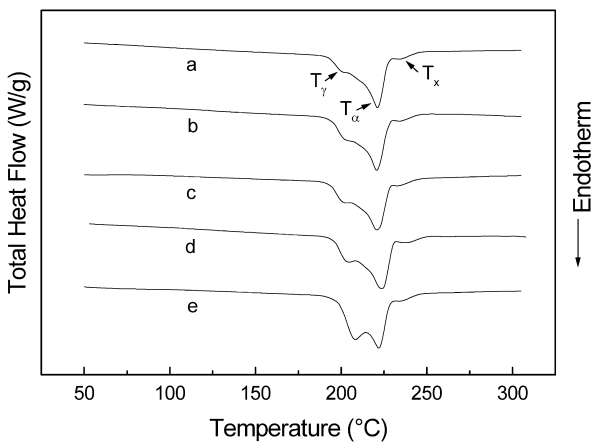

Fig. 4. MDSC traces of PA6LSN annealed at 190 °C for (a) 10 min, (b) 30 min, (c) 60 min, (d) 120 min and (e) 240 min.

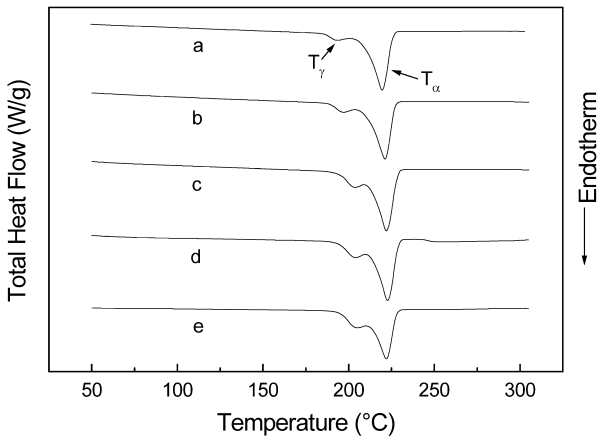

Fig. 5. MDSC traces of pure PA6 annealed at 190 °C for (a) 10 min, (b) 30 min, (c) 60 min, (d) 120 min and (e) 240 min.

process [33], and consequently the dominant α-form crystals in PA6SLN are able to rearrange to an increasingly favoured γ-phase conformation because of the thermal activation provided by annealing and this phase conversion will became more prominent when enough annealing time is given. It seems that the thermal history introduced through our annealing cycle decreases the processing effect that favoured the formation of α-form crystal, and this effect becomes significantly more prominent when the nano-silicate particles are present.

The DSC traces of both PA6LSN and PA6, annealed at 230 °C, are illustrated in Figs. 8 and 10, respectively. It is worthwhile to note from Fig. 8 that the melting peaks of γ-form crystals are greatly enhanced while the melting peaks corresponding to α-form crystals are reduced to only a much less pronounced shoulder and finally disappeared as the annealing times exceeded 120 min. The dominant fractions of the γ-phase in the PA6LSN samples annealed at 230 °C as compared with those annealed at 190 °C suggest that γ-form crystal forms more readily during melt state annealing than annealing in the solid state. This is because, when PA6LSN is annealed in the melt state, heterophase nucleation effect of nano-silicate particles may

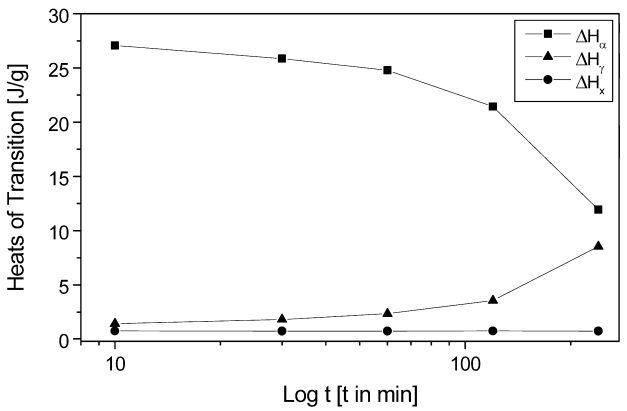

Fig. 6. Relationship between enthalpy of transition (ΔH) and logarithmic time (log t) for PA6LSN system.

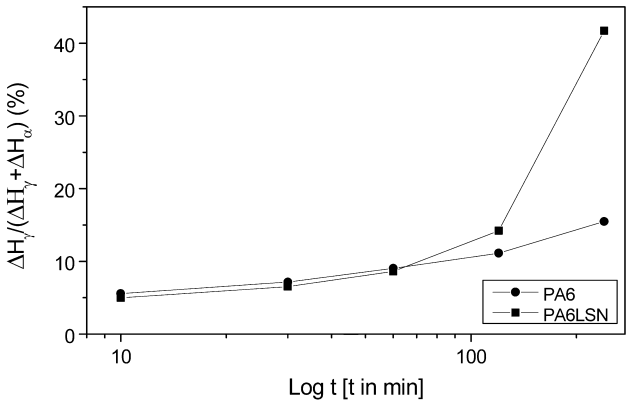

Fig. 7. Changes in the content of γ-phase as a function of annealing time (annealed at 190 °C).

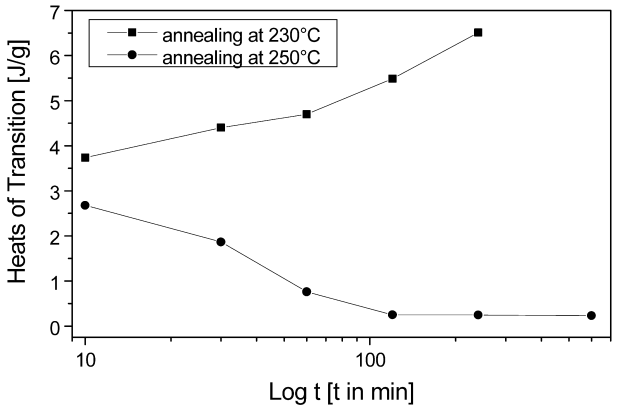

Fig. 9. Changes in enthalpy of transition (ΔH_x) as a function of annealing time at different annealing temperatures.

play an important role in the small molten PA6 droplets, which are more favourable for the formation of γ-form crystals. Similar result was also observed in the PA6LSN sample annealed in melt state at 250 °C. Furthermore, it can also be seen from Fig. 8 that the values of T_γ and T_α remained fairly constant independent of annealing time at both 230 and 250 °C, but the high-temperature endothermic peak (>230 °C), T_x, shifted to higher temperature with increasing annealing time. Meanwhile, its enthalpy of transition, ΔH_x, increased steadily with increasing annealing time (see Fig. 9). The increase in both T_x and ΔH_x appears to indicate that this annealing temperature could lead to the formation of more perfect structures for the high melting temperature structures.

For neat PA6 annealed at 230 °C (Fig. 10), however, very different DSC thermograms were obtained, where the α-crystal is still the most predominant phase and the melting peak corresponding to γ-form crystals is observed only as a small shoulder. This can be attributed to the fact that annealing in the melt state could provide more thermal activation to allow PA6 molecules to arrange themselves into a more stable chain conformation, which results in the formation of the most favourable packing arrangement with lower energy crystal conformation. Hence thermodynamically stable α-phase is expected as the predominant phase.

The DSC thermograms of both neat PA6 and PA6LSN, annealed at 250 °C (melt-state annealing II) for various durations, are shown in Figs. 11 and 12, respectively. It is clear from Fig. 11 that peak temperature T_α of neat PA6 specimens showed no change and the peak area also remain virtually constant after the specimen were annealed at 250 °C for different periods of time. This suggests that annealing at 250 °C has no significant effects on the structure of neat PA6 similar to that observed for neat PA6 annealed at 230 °C. But for PA6LSN, the following observations are worth noting in Fig. 12. (1) After being annealed at 250 °C for different durations, the γ-form crystal becomes the absolutely dominant crystalline phase and almost no α-phase was detected. On the other hand, the peak temperatures, T_γ, remain fairly constant and appear unaffected by annealing at this temperature. This again is probably due to the presence of layer-silicate which induced the heterophase nucleation of γ phase as well as due to the relatively high cooling rate (40 °C/min) both favoring the γ phase formation. (2) Peak temperature of the new endotherm, T_x, and its associated melt enthalpy, ΔH_x,

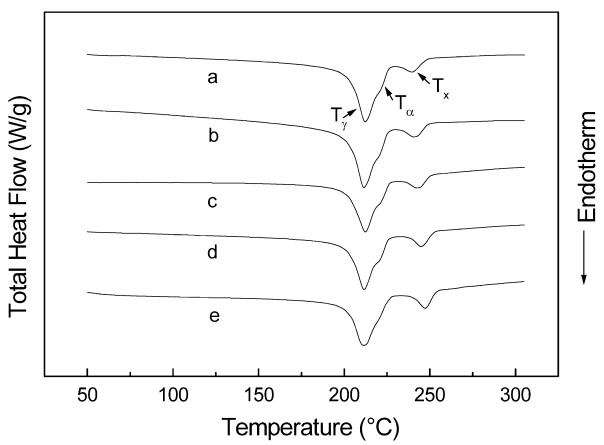

Fig. 8. MDSC traces of PA6LSN annealed at 230 °C for (a) 10 min, (b) 30 min, (c) 60 min, (d) 120 min and (e) 240 min.

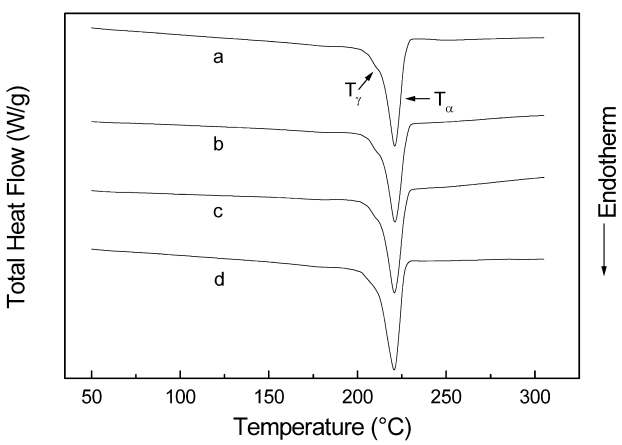

Fig. 10. MDSC traces of pure PA6 annealed at 230 °C for (a) 30 min, (b) 60 min, (c) 120 min and (d) 240 min.

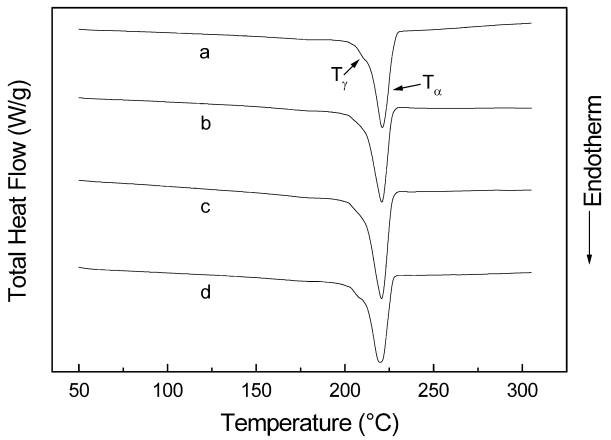

Fig. 11. MDSC traces of pure PA6 annealed at 250 °C for (a) 30 min, (b) 60 min, (c) 120 min and (d) 240 min.

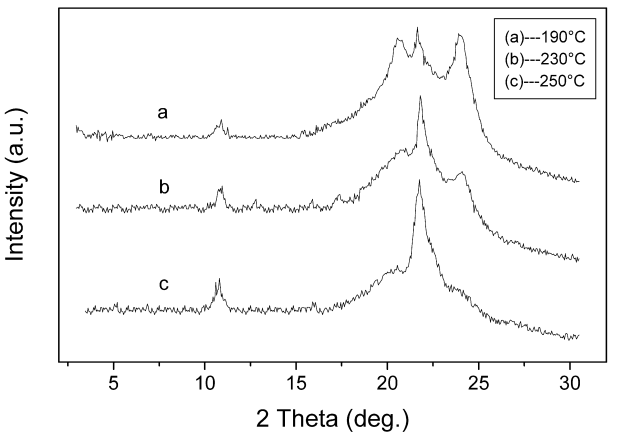

Fig. 13. WAXD patterns of PA6LSN sample annealed at (a) 190 °C, (b) 230 °C and (d) 250 °C for 240 min.

decreased gradually with increasing annealing time up to 120 min. However, when the annealing time exceeded 120 min, no further change was observed in the T_x and ΔH_x even for a much longer annealing time such as 10 h (see Fig. 9). Most interestingly, when the 10 h-annealed sample at 250 °C was re-annealed at 230 °C, T_x and ΔH_x were found to be able to recover to the level observed for samples annealed at 230 °C in the first instance.

In order to further confirm the origin of this high-temperature melting peak, XRD analysis was carried out using the annealed samples which were prepared using the same procedures as for the DSC measurements. Fig. 13 illustrates wide-angle X-ray diffraction scans of the as-received PA6LSN sample annealed for 240 min at 190, 230 and 250 °C respectively. The XRD results agree well with the DSC observations. However, in combination with the XRD result of Fig. 3, it should be noted that no new reflection peak is detected both in the annealed and non-annealed PA6LSN samples except for peaks corresponding to the α-phase and γ-phase. This means that it is unlikely that no new crystalline structure is formed in the PA6LSN samples in this case. It is speculated that this new melting peak might be related to the melting of PA6 fine lamellae formed in the microenvironment on layered-silicate surface. It was found by Okazaki and Wunderlich through study on the melting behaviors of PET that there was a 'molecular nucleation' process when chains or chain segments melt near or on high-melting crystals, these molecular chains or chain segments can nucleate and recrystallize on these existing unmelted crystals with negligible cooling [34,35]. Following this line of reasoning, silicates can be considered as 'high-melting crystals', some of the PA6 molecules or chain segments tethered on the surface of silicates by strong (interfacial) ionic interactions [36] might be able to rearrange their chains or chain segments to a more ordered form during melting process. As a result, some fine lamellae could be formed in the confined environment on the surface of layered-silicate. These fine lamellae can be also regarded as potential nuclei of further crystallization. Indeed, Varlot et al. [17] have speculated the existence of the oriented PA6 lamellae relative to the organoclay sheets in PA6/silicate nanocomposites.

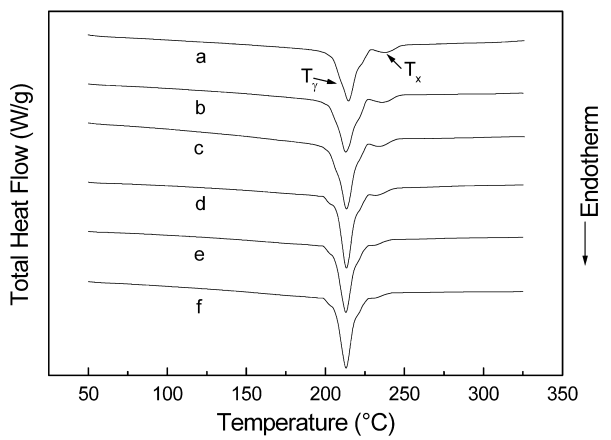

Fig. 12. MDSC traces of PA6LSN annealed at 250 °C for (a) 10 min, (b) 30 min, (c) 60 min, (d) 120 min, (e) 240 min and (f) 600 min.

Two factors might affect the existence of fine lamellae, one is the specific polymer-surface interaction (adhesion) between the PA6 molecules and silicate, and another is the space for the rearrangement of PA6 molecules. Since γ-crystals have the larger distance (0.933 nm) compared to 0.801 nm of α-crystals [37], they will be able to provide more space for the silicate layer in between the sheets of PA6 chains without much straining. Accordingly, the PA6 fine lamellae tethered on silicate surface could also obtain more space for arrangement. Little change in both T_x and ΔH_x for PA6LSN samples with increasing annealing time at 190 °C seems to indicate that this isothermal annealing temperature is not high enough for fine lamellae to achieve a better arrangement although the conversion from the γ-phase to the α-phase can provide more space. As the annealing temperature was elevated to 230 °C, not only was the more space provided due to the γ-phase becoming the absolutely dominant crystalline phase, but also could the fine lamellae achieve a better arrangement because of enough thermal activation provided by annealing. Therefore,

it is reasonable to find that the values of both ΔH_x and T_x associated with high-temperature endothermic peak increased with increasing annealing time. When the annealing temperature was further increased to 250 °C, some fine lamellae attached on the surface of silicates could be destroyed and the amount left would become less and less with increasing annealing time. Hence, the value of ΔH_x decreased with increasing annealing time. It was initially believed that when enough annealing time was given at 250 °C, this high-temperature endothermic peak would completely disappear eventually. The question is why it did not disappear even for long annealing duration up to 10 h, and ΔH_x leveled off as the annealing time exceeding 120 min. The most plausible reason for such behavior might be related to the formation of new fine lamellae during the DSC re-scan carried out at 5 °C after annealing and cooling. Nevertheless, a deeper understanding of this phenomenon requires further studies which are being carried out. We strongly believe that such interesting phenomenon observed in the present study is related to the unique structure and carefully controlled synthesis conditions for this in situ polymerized reactor grade PA6 nanocomposite based on synthetic silicate [24,25].

4. Conclusions

In this work, the differences in polymorphism and thermal behavior between PA6LSN and PA6 have been comparatively studied and the effect of thermal history on the time evolution of the polymorphic structure of PA6LSN and neat PA6 was also investigated. The polymorphic behavior and thermal properties of PA6LSN were found to strongly depend on the thermal history. Annealing at 190 °C followed by controlled fast cooling caused significant changes in polymorphism of these materials. However, the effect is much more prominent in PA6LSN than in neat PA6 especially for the longer annealing time. It seems that annealing suppressed the processing effect that favored the formation of α-form crystal, and conversely, increased the effect of silicate particles which promoted the formation of γ-phase. On the other hand, annealing in the melt state has lead to the γ crystal becoming the dominating crystalline phase in PA6LSN sample and higher annealing temperature would amplify this phenomenon, probably due to a strong heterophase nucleation effect. For neat PA6 annealing in the melt state, however, the α crystal is still the most predominant phase independent on the annealing temperature. The differences in polymorphism between pure PA6 and PA6LSN reflected the complexity of the melting behavior of PA6LSN system. Furthermore, the appearance of new endothermic peak in PA6LSN system is attributed to the melting of PA6 fine lamellae formed in the confined environment on the surface of silicate. The peak temperature and enthalpy of this new endotherm were enhanced steadily when annealing was carried out at 230 °C but suppressed gradually when annealed at 250 °C. It is clear that this new melting peak is strongly dependent on the thermal history.

Acknowledgements

The authors would also like to thank Dr Thomas S. Ellis of Delphi, USA and Professor Albert F. Yee of University of Michigan for supplying the samples and for their useful discussion.

References

[1] Okada A, Kawasumi M, Kurauchi T, Kamigaito O. Polym Prepr 1987; 28:447.
[2] Usuki A, Kojima Y, Kawasumi M, Okada A, Fukushima Y, Kurauchi T, Kamigaito O. J Mater Res 1993;8:1179.
[3] Burnside SD, Giannelis EP. Chem Mater 1995;7:1597.
[4] Lee DC, Jang LW. J Appl Polym Sci 1998;68:1997.
[5] Lincoln DM, Vaia RA, Wang Z, Hsiao BS, Krishnamoorti R. Polymer 2001;42:9975.
[6] Yano K, Usuki A, Okada A, Kurauchi T, Kamigaito O. J Polym Sci 1993;A31:2493.
[7] Yano K, Usuki A, Okada A. J Polym Sci 1997;A35:2289.
[8] Gilman JW. Appl Clay Sci 1999;15:31.
[9] Morgan AB, Gilman JW, Harris RH, Jackon CL, Wilkie CA, Zhu J. Polym Mater Sci Engng 2000;83:53.
[10] Komarneni S. J Mater Chem 1992;2:1219.
[11] Hill PG, Foot PJS, Davis R. Synth Met 1996;76:289.
[12] Mark JE. Polym Engng Sci 1996;36:2905.
[13] Lebaron PC, Wang Z, Pinnavaia TJ. Appl Clay Sci 1999;5:11.
[14] Liu LM, Qi ZN, Zhu XG. J Appl Polym Sci 1999;71:1133.
[15] Mathias LJ, Davis RD, Jarrett WL. Macromolecules 1999;32:7958.
[16] Wu TM, Liao CS. Macromol Chem Phys 2000;201:2820.
[17] Varlot K, Reynaud E, Kloppfer MH, Vigier G, Varlet J. J Polym Sci Polym Phys 2001;39:1360.
[18] Wu TM, Chen EC, Liao CS. Polym Engng Sci 2002;42:1141.
[19] LeBaron PC, Wang Z, Pinnavaia TJ. Appl Clay Sci 1999;15:11.
[20] Vaia RA, Price G, Ruth PN, Nguyen HT, Lichtenhan J. Appl Clay Sci 1999;15:67.
[21] Kojima Y, Matsuoka T, Takahashi H, Kurauchi T. J Mater Sci Lett 1993;12:1714.
[22] Okada A, Fukushima Y, Kawasumi M, Inagaki S, Usuki A, Sugiyami S, Kurauchi T, Kamigaito O. US Patent NO: 4739007; 1998.
[23] Kata M, Usuki A. In: Pinnavaia TJ, editor. Polymeric-clay nanocomposites. England: JWS; 2000.
[24] Ellis TS, D'Anglelo S. J Appl Polym Sci 2003;90:1639.
[25] Ellis TS. Polymer 2003;44:6443.
[26] Illers HK, Haberkorn H, Simak P. Makromol Chem 1972;158:285.
[27] Cheng LP, Lin DJ, Yang KC. J Membr Sci 2000;172:157.
[28] Illers HK, Haberkorn H. Makromol Chem 1971;142:31.
[29] Murthy NS, Curran SA, Aharoni SM, Minor H. Macromolecules 1991;24:3216.
[30] Samon JM, Schultz JM, Wu J, Hsiao B, Yeh F, Kolb R. J Polym Sci Polym Phys 1999;37:1277.
[31] Schultz JM, Hsiao B, Samon JM. Polymer 2000;41:8887.
[32] Ramesh C, Bhoje GE. Macromolecules 2001;34:3308.
[33] Khanna YP. Macromolecules 1992;25:3298.
[34] Okazaki I, Wunderlich B. Macromol Rapid Commun 1997;18:313.
[35] Okazaki I, Wunderlich B. Macromolecules 1997;30:1758.
[36] Vogelsong DC, Pearce EM. J Polym Sci 1960;45:546.
[37] Xenopoulos A, Clark ES. In: Kohan MI, editor. Nylon plastics handbook. New York: Hanser Publishers; 1995.